Draft version January 23, 2015
Preprint typeset using LaTeX style emulateapj v. 5/2/11

arXiv:1501.05312v1 [astro-ph.GA] 21 Jan 2015

OVERTURNING THE CASE FOR GRAVITATIONAL POWERING IN THE PROTOTYPICAL COOLING Lyα NEBULA

Moire K. M. Prescott[1], Ivelina Momcheva[2], Gabriel B. Brammer[3], Johan P. U. Fynbo[1], Palle Møller[4]

Draft version January 23, 2015

ABSTRACT

The Nilsson et al. (2006) Lyα nebula has often been cited as the most plausible example of a Lyα nebula powered by gravitational cooling. In this paper, we bring together new data from the Hubble Space Telescope and the Herschel Space Observatory[a] as well as comparisons to recent theoretical simulations in order to revisit the questions of the local environment and most likely power source for the Lyα nebula. In contrast to previous results, we find that this Lyα nebula is associated with 6 nearby galaxies and an obscured AGN that is offset by $\sim 4'' \approx 30$ kpc from the Lyα peak. The local region is overdense relative to the field, by a factor of ∼10, and at low surface brightness levels the Lyα emission appears to encircle the position of the obscured AGN, highly suggestive of a physical association. At the same time, we confirm that there is no compact continuum source located within $\sim 2\text{-}3'' \approx 15\text{-}23$ kpc of the Lyα peak. Since the latest cold accretion simulations predict that the brightest Lyα emission will be coincident with a central growing galaxy, we conclude that this is actually a strong argument *against*, rather than for, the idea that the nebula is gravitationally-powered. While we may be seeing gas within cosmic filaments, this gas is primarily being lit up, not by gravitational energy, but due to illumination from a nearby buried AGN.

Subject headings: galaxies: evolution — galaxies: formation — galaxies: high-redshift

1. INTRODUCTION

There has been a long-standing debate about the power source responsible for radio-quiet Lya nebulae (or "Lyα blobs"). Unlike extended Lyα halos observed around many radio galaxies and quasars, radio-quiet Lyα nebulae do not always have an obvious single source of ionizing photons in their midst. Various explanations have been proposed: for example, shock-heating in galactic superwinds (Taniguchi & Shioya 2000; Taniguchi et al. 2001; Mori et al. 2004), photoionization from nearby galaxies and AGN (e.g., Cantalupo et al. 2005; Geach et al. 2009; Kollmeier et al. 2010; Prescott et al. 2012b; Overzier et al. 2013), and resonant scattering of centrally produced Lyα photons (e.g., Møller & Warren 1998; Laursen & Sommer-Larsen 2007; Zheng et al. 2011; Steidel et al. 2011; Hayes et al. 2011). One final explanation is that Lyα nebulae are powered by gravitational cooling radiation within cold accretion streams. This possibility has received substantial theoretical attention over the past few years, motivated in large part by evidence from numerical simulations that a cold mode of accretion could play an important if not dominant role in fueling galaxy formation (e.g., Keres et al. 2005; Dekel et al. 2009).

Against this backdrop, Nilsson et al. (2006) reported the discovery of a Lyα nebula at $z \approx 3.157$ in the GOODS-S field. Intriguingly, the deep GOODS imaging showed no associated continuum detections in any band, from the X-rays to the infrared. The photometric redshifts available at the time indicated that none of the nearby galaxies were likely to be at the redshift of the nebula nor would they be able to provide sufficient energy to power the nebula even if they were. Based on the lack of any obvious source of ionizing photons and on the similarity between the observed Lyα surface brightness profile and early predictions from cold accretion models, the authors suggested that this system could be powered by cooling radiation. Since then, discussions of the range of power sources observed for Lyα nebulae typically include a reference to this system as the clearest observational example of a "cooling" Lyα nebula (e.g., Smith et al. 2008; Dijkstra 2009; Adams et al. 2009; Rasmussen et al. 2009; Laursen et al. 2009; Yang et al. 2010; Goerdt et al. 2010; Weijmans et al. 2010; Colbert et al. 2011; Erb et al. 2011; Cen & Zheng 2013; Laursen et al. 2013; Tamura et al. 2013; Yajima et al. 2013).

However, a number of things have changed substantially since the initial discovery of this Lyα nebula. On the observational side, grism spectroscopy, deeper X-ray catalogs, and additional imaging - spanning the rest-frame optical to far-infrared - have become available in the GOODS-S field thanks to the Early Release Science program (Windhorst et al. 2011), the 2 Ms and 4 Ms Chandra Deep Field-South (CDF-S) Surveys (Luo et al. 2008; Xue et al. 2011), GOODS-Herschel (Elbaz et al. 2011), and HerMES (Levenson et al. 2010; Oliver et al. 2012), allowing for significant improvements to both photometric and spectroscopic redshift measurements in the region. In addition, some observational studies of other Lyα nebulae have shown that the Lyα emission can actually be offset substantially (∼10s of

---

[1] Dark Cosmology Centre, Niels Bohr Institute, University of Copenhagen, Juliane Maries Vej 30, 2100 Copenhagen Ø, Denmark; mkmprescott@dark-cosmology.dk
[2] Department of Astronomy, Yale University, New Haven, CT 06511, USA
[3] Space Telescope Science Institute, 3700 San Martin Drive, Baltimore, MD 21218, USA
[4] European Southern Observatory, Karl-Schwarzschildstrasse 2, D-85748 Garching bei München, Germany

[a] Herschel is an ESA space observatory with science instruments provided by European-led Principal Investigator consortia and with important participation from NASA.

kpc) from associated galaxies and obscured AGN at the same redshift (Prescott et al. 2009, 2012a,b, 2013; Yang et al. 2014). On the theoretical side, simulations of "cooling" Lyα nebulae have been carried out with greater and greater sophistication over the past few years (e.g., Goerdt et al. 2010; Faucher-Giguère et al. 2010; Rosdahl & Blaizot 2012). In light of the new observational data and more advanced numerical simulations, the time is ripe to return to this system and take another look at its local environment and most likely power source.

In this paper, we revisit the following questions: (1) does the Lyα nebula have any associated galaxies, and (2) is it likely powered by cold accretion? We describe the datasets used in this work in Section 2, and we study the neighborhood of the Lyα nebula in Section 3. In Section 4 we discuss the most likely powering mechanism responsible for the Lyα nebula, taking into account updated predictions from numerical simulations. Section 5 highlights some implications of this work for the larger class of Lyα nebulae, and we conclude in Section 6. We assume the standard ΛCDM cosmology (Ω_M=0.3, Ω_Λ=0.7, h=0.7); the angular scale at $z = 3.156$ is 7.58 kpc/$''$. All magnitudes are in the AB system (Oke 1974).

2. DATA

This paper builds on the large number of existing datasets and catalogs with coverage of the GOODS-S field.

2.1. *Lyα Narrowband Imaging and Spectroscopy*

The original Lyα imaging was obtained as part of a survey for Lyα-emitting galaxies using FORS1 on the VLT 8.2 m telescope Antu and a standard narrowband filter (λ_c=5055Å; $FWHM$=59Å, corresponding to Lyα at $z = 3.126 - 3.174$). The nebula emission was confirmed to be Lyα at $z = 3.157$ via follow-up spectroscopy from VLT/FORS1, which showed a single emission line with the classic asymmetric profile expected for high redshift Lyα emission and no detections of the other strong lines that would have been expected from a low redshift interloper. Details on the Lyα imaging and follow-up spectroscopy are given in the original survey papers (Nilsson et al. 2006, 2007).

2.2. *HST Imaging and Grism Spectroscopy*

The Lyα nebula is located within the GOODS-S/ERS field. The area was originally observed as part of the GOODS South program in the ACS $BVRiz$ filters (Giavalisco et al. 2004; Dickinson et al. 2004). The same region was more recently targeted as part of the WFC3/ERS observations in Cycle 17 following the installation of WFC3 during Servicing Mission 4 (GO/DD: 11359, 11360; PI: R. O'Connell Windhorst et al. 2011). Images were acquired in the $F098M$, $F125W$ and $F160W$ filters, using two orbits in each filter. Additional shallower imaging in the $F140W$ filter was done to provide a direct-image reference for a single pointing of ERS $G141$ grism observations (discussed below). The $F140W$ observations partially overlap with the footprint of the 3D-HST program (GO: 12177; PI: van Dokkum) which also provides $F140W$ images over a larger area. The GOODS-S/ERS field has been observed by an array of additional ground- and space-based facilities. In this work, we make use of WFC3-IR $F125W$, $F140W$, and $F160W$ imaging and the WFC3-detected photometric catalog of the GOODS-S field compiled by Skelton et al. (2014). The WFC3 imaging represents a significant improvement over the ground-based J and H-band data available previously, as it provides high resolution imaging coverage near the critical 4000Å break, and enabling much more robust photometric redshift estimates; see Skelton et al. (2014) for further information. We make use of the photometric redshift catalog from Skelton et al. (2014), which is based on the code EAzY (Brammer et al. 2008), and morphological measurements for galaxies in the region taken from the CANDELS morphological catalog (van der Wel et al. 2012).

The Lyα nebula is serendipitously located in the one and only grism pointing observed as part of the ERS program (Windhorst et al. 2011, GO/DD: 11359, 11360; PI: R. O'Connell) The observations were done in both the $G102$ and $G141$ grisms, spanning $0.8 - 1.2\ \mu m$ and $1.1 - 1.7\ \mu m$, respectively. The two grism provide resolutions of $R \sim 210$ and 130. The pointing was observed for two orbits with each grism. In this work we use only the $G141$ grism observations, which covers the [O II]λ3727 emission line out to $z \approx 3.2$, as none of the objects relevant to this work have significant detections in the $G102$ spectra. The grism data were reduced by the 3D-HST team in a manner similar to that described in Brammer et al. (2012). Further details on the extraction and redshift-fitting methods will be presented in Momcheva et al. (in prep.).

2.3. *Mid- and Far-Infrared Data*

The original paper presented Spitzer IRAC and MIPS imaging of the field (Nilsson et al. 2006, their Figure 2). At longer wavelengths, Herschel PACS and SPIRE coverage of the field now exists from GOODS-Herschel and HerMES (Elbaz et al. 2011; Oliver et al. 2012). In addition, improvements have been made in extracting accurate IRAC/MIPS photometry properly accounting for source blending and the complex PSF of these instruments, and there has been extensive work on the best way to use IRAC/MIPS colors to distinguish AGN from star-forming galaxies (Stern et al. 2005; Lacy et al. 2004, 2007; Donley et al. 2008, 2012).

In this work, the mid- and far-infrared photometry are taken from the GOODS-Herschel catalog, which includes measurements from the GOODS-Spitzer Legacy Survey (Spitzer/IRAC+MIPS; P.I. Mark Dickinson) and the GOODS-Herschel Survey (Herschel/PACS; Elbaz et al. 2011), accessed via HeDaM.[5] Source positions in the GOODS-Herschel catalog were determined first using a weighted average of the 3.6 and 4.5 micron images, and then empirical PSFs at these source locations were fit to the mid- and far-infrared maps in order to determine the flux for each object and account for source blending. Further details are given in the GOODS-Herschel release documentation.[6]

The field has been observed in the far-infrared with Herschel/SPIRE as part of HerMES (Oliver et al. 2012; Levenson et al. 2010; Roseboom et al. 2010, 2012). In this work, we make use of Herschel/SPIRE photometric measurements from the MIPS 24μm-matched catalog developed by the HerMES Team (HerMES Team, private communication).

---

[5] http://hedam.lam.fr

[6] http://hedam.lam.fr/GOODS-Herschel/goodss-data.php

2.4. *Chandra X-ray Coverage*

Since the original paper, the Chandra X-ray coverage of GOODS-S has improved substantially from the original Chandra Deep Field-South 1 Ms survey, first by a factor of two and then by a factor of four in total exposure time. The resulting Chandra Deep Field-South 2 Ms and 4 Ms survey catalogs (Luo et al. 2008; Xue et al. 2011) provide a sample 740 X-ray detected sources down to limiting on-axis fluxes of $\approx 3.2\times10^{-17}$, 9.1×10^{-18}, and 5.5×10^{-17} erg s^{-1} cm^{-2} for the 0.5-8 keV full band, the 0.5-2 keV soft band, and the 2-8 keV hard band, respectively.

3. REVISITING THE NEIGHBORHOOD

Nilsson et al. (2006) listed 8 objects within a $10''$ radius that had detections in at least 8 photometric bands, and an additional 8 nearby sources that were detected in only a subset of those bands, too few for reliable photometric redshifts to be estimated. Of the 8 sources with derived photometric redshifts, they presented projected distances and photometric redshifts in their Table 2. None appeared to be precisely at the Lyα nebula redshift, although four of these sources were consistent with it to within the relatively large quoted errors (Sources 3, 5, 6, and 8). Two of these sources were not discussed further (Sources 5 and 8). The authors argued that Source 3 was unlikely to power the nebula, even if it were at the correct redshift, because it did not appear to emit enough ionizing photons. Finally, in the case of Source 6, a mid-infrared source that was detected in the IRAC and MIPS bands, they concluded the object was most likely an unassociated starburst galaxy at high redshift ($z \approx 5.5$) based on comparisons to Spitzer IRAC/MIPS color-color diagnostic diagrams from Ivison et al. (2004).

Using the new and improved datasets described in the previous section, we revisit the following question: is this Lyα nebula truly a line-emitting nebula without any associated galaxies?

3.1. *Searching for Associated Galaxies*

3.1.1. *Photometric Redshifts*

Figure 1 shows a stack of the WFC3-IR/$F125W$, $F140W$, and $F160W$ imaging in the vicinity of the Lyα nebula, shown as contours,[7] while Figure 2 shows the individual bands. Using the 3D-HST/CANDELS photometric redshift catalog (Skelton et al. 2014), we select sources that lie within a $10''$ radius of the Lyα nebula. Figure 3 shows the distribution of photometric redshifts in this region, both as a histogram and as a sum of the individual galaxy P(z) distributions. The photometric redshift distribution shows two main peaks: one at $z \approx 1$ and one around $z \approx 3.1$, i.e., roughly the redshift of the nebula. Formally, 6 sources within this local region ($R < 10''$) have photometric redshifts within $\Delta z \pm 0.15$ of the nebula redshift; the positions and photometric redshifts of these "photometric redshift members" are given in Table 1. We plot the selected photometric redshift members on the HST imaging (Figure 2, right-hand panel). Of these 6 sources, photometric redshift estimates for two (Source 3 and 8) were given in the original paper; the new photometric redshifts for these sources are consistent with the previous estimates, given the quoted error bars. The photometric redshifts of the remaining sources were previously unknown.

We note that while photometric redshifts will clearly be less accurate and more susceptible to biases, especially at fainter magnitudes, relative to true spectroscopic redshifts, a recent study of a suite of photometric redshift codes found that individual codes based on EAzY (Brammer et al. 2008) do reasonably well in terms of their reported errors (i.e., corresponding to the width of the reported P(z) peak), underestimating by about 5-15% (Dahlen et al. 2013). The scatter (σ_0 = rms[Δz/(1+z)]) between the spectroscopic redshift and the median photometric redshift was found to increase from $\sigma_0 = 0.04$ at $m_H < 24$ mag to 0.09 at $m_H \sim 26$ mag, while the outlier fraction increased from about 10% to 20%. Thus by using a redshift window of $\Delta z \pm 0.15$, we can be reasonably confident that we are primarily selecting galaxies at the redshift of the nebula even at these fainter magnitudes.

To test the significance of the observed photometric redshift peak coincident with the nebula, we redid the analysis for 10000 random apertures drawn from the entire GOODS-S field. We find that at $z \sim 3$, it is not common to find a peak in the photometric redshift distribution that is as strong as what is seen at the position of the Lyα nebula: formally there is a 2.0% chance of randomly selecting a region with comparable area under the summed P(z) distribution, or a 0.4% chance of randomly selecting a region with at least 6 galaxies with best fit photometric redshifts within $\Delta z \pm 0.15$ of the nebula redshift.

Interestingly, the very faint source visible in the $F160W$ image that is located closest to the peak of the Lyα emission turns out to be one of the $z \approx 1$ sources (labeled as Galaxy 'F' in Figure 1). The measured SED and P(z) derived by EAzY for this source show that it is well-described by the EAzY fit at $z = 0.91$ with a stellar mass of $\approx 1.2 \times 10^8$ M$_\odot$, and that it is inconsistent with either an AGN or starburst template at the nebula redshift (Figures 4-5). Thus, we confirm that there does not appear to be any associated continuum source within $\sim$2-3$''\approx$15-23 kpc of the peak of the Lyα emission.

We note that gravitational lensing from the foreground sources at $z \approx 1$ should only have a minimal effect on the nebula. If we take all galaxies in the local vicinity that have photometric redshifts within ±0.15 of $z = 1$, the total stellar mass derived from the SED fitting is $\approx 3 \times 10^{10}$ M$_\odot$, with the brighter (and presumably more massive) $z \approx 1$ sources being located about $5''$ to the northwest of the nebula (Figure 2, middle panel). If the corresponding total mass of the foreground structure is of order 3×10^{11} M$_\odot$, the expected Einstein radius would be $\approx 0.2''$, insignificant compared to the full extent of the Lyα emission, and the magnification at the position of the Lyα peak would only be about 3%. If we consider only the source located closest to the center (Galaxy 'F', with a stellar mass of 1.2×10^8 $M_\odot$), the expended Einstein radius would be $\approx$0.05″. Thus, neither the large scale morphology nor the surface brightness of the nebula is significantly affected by gravitational lensing from the $z\approx1$ sources.

---

[7] We note that the surface brightness levels for the contours plotted in Nilsson et al. (2006) appear to have been stated incorrectly in the caption of their Figure 1.

3.1.2. *Grism Redshifts*

We next searched the grism redshift catalog for sources with grism redshifts consistent with the nebula. We find that one of the 6 photometric redshift neighbors (Source 3) shows a weak [OII] detection (Figure 6). This corresponds to a measured grism redshift of $z_{grism} = 3.153^{+0.019}_{-0.004}$ (Table 1), consistent with the photometric redshift ($z_{phot} = 3.206^{+0.065}_{-0.058}$) and with the nebula redshift measured from the Lyα emission line ($z_{Ly\alpha} = 3.157$). Neither the extended nebula itself nor any of the other galaxy members, which are all much fainter in $F160W$ continuum magnitude than Source 3, show a line detection in either the $G102$ or $G141$ grism spectroscopy.

3.1.3. *Source 6 - The IRAC/MIPS Source*

We take a second look at Source 6, the mid-infrared source first identified in the Spitzer IRAC and MIPS data. We plot the full SED including the original GOODS-S imaging and Spitzer data, as well as the new HST/WFC3-IR imaging and measurements from Herschel/PACS and SPIRE (Figure 7). The source shows diffuse emission in the WFC3-IR imaging, but it is below the detection limit in the combined WFC3 detection image used in Skelton et al. (2014); therefore, we measure the photometry in these bands using a 2.4″ radius aperture at the position of Source 6, as determined from the IRAC 3.6 and 4.5μm imaging. The IRAC/MIPS photometry and Herschel PACS upper limits are taken from the GOODS-Herschel catalog (Elbaz et al. 2011), and the Herschel SPIRE measurements are from HerMES (HerMES Team, private communication). We note that Source 6 is not detected in either the WFC3/$G102$ or $G141$ grism data.

Using these updated measurements, we derive the following MIR colors (relevant for the Ivison et al. (2004) color-color selection): $S_{24.0}/S_{8.0} = 9.959 \pm 2.792$ and $S_{8.0}/S_{4.5} = 2.160 \pm 0.380$. While Nilsson et al. (2006) suggest Source 6 is an obscured starburst at an approximate redshift of $z \approx 5.5$ based on its MIR colors, the MIR color measurements taken from the GOODS-Herschel catalog place Source 6 elsewhere in the Ivison et al. (2004) color space, much higher in $S_{24.0}/S_{8.0}$ and therefore much closer to the Mrk231 (i.e., AGN) locus. It is possible that the original measurements did not adequately account for source blending and the complex MIPS PSF, yielding an incorrect 24μm flux for this relatively faint MIR source that happens to lie near the Airy ring from a brighter neighboring galaxy.

Furthermore, AGN selection based on MIR colors has been explored in great detail since the time of the original paper (Stern et al. 2005; Lacy et al. 2004, 2007; Donley et al. 2008, 2012). The measured MIR colors relevant for these color-color diagnostics are: $log(S_{8.0}/S_{4.5}) = 0.335^{+0.070}_{-0.084}$ and $log(S_{5.8}/S_{3.6}) = 0.242^{+0.107}_{-0.142}$. These measurements place Source 6 solidly within the AGN color selection window of Lacy et al. (2004, 2007), and within the more recent IRAC power-law AGN selection box of Donley et al. (2012). From the mid-infrared colors, Source 6 is therefore very likely an obscured AGN and not a starburst galaxy. The Herschel detections are susceptible to source confusion but suggest that there may be an additional cool dust component, e.g., emission from the host galaxy.

It is true that Source 6 was not detected in the deep 1 Ms CDF-S X-ray imaging, as pointed out in the original paper. We find that the source is still not detected in the more recent 2 Ms and 4 Ms CDF-S catalogs (Luo et al. 2008; Xue et al. 2011). However, a study of power-law IRAC selected AGN candidates in the 2 Ms Chandra Deep Field-North (CDF-N) X-ray imaging showed 23% (35%) were not detected above 3σ (5σ) in any X-ray band (Donley et al. 2007), while stacking of the X-ray non-detected sources still showed evidence for hard emission consistent with AGN rather than star formation powering (Donley et al. 2012). Thus, it appears that the lack of an X-ray detection from Source 6, even in deep Chandra data, cannot necessarily be used to rule out the presence of an intrinsically luminous AGN that is simply heavily obscured at X-ray wavelengths.

Based on the photometry derived from the original GOODS-S HST and Spitzer/IRAC data and the new ERS imaging, we use the photometric redshift code EAzY (Brammer et al. 2008) to estimate a photometric redshift for Source 6. Including the IRAC photometric points and the standard EAzY star-forming galaxy templates results in a redshift of $z \approx [3.2 - 5.6]$, similar to what was found in the original paper. However, if Source 6 is an obscured AGN, as we have argued, the IRAC bands will be dominated by AGN emission, making a photometric redshift estimate based on only star-forming templates highly unreliable. The photometric redshift estimate will be skewed to higher redshifts ($z \gtrsim 4$) by the need to fit the bright 8.0μm point with the brightest part of the star-forming SED, i.e., the peak located at restframe $\sim$1.6μm. Adding the Mrk 231 AGN template to EAzY and including both the IRAC and MIPS detections (the Herschel detections and upper limits being excluded due to possible source confusion) yields a slightly lower redshift range of $z \approx [2.8, 5.2]$ that straddles the redshift of the Lyα nebula. This estimate is not very robust, since fitting the power-law MIR SED with an AGN template does not contribute a lot of discriminatory power, but it illustrates that $z \approx 3.2$ is a plausible redshift for Source 6.

3.2. *Spatial Distribution of the Associated Galaxies and the Larger Scale Lyα Emission*

The spatial distribution of likely members relative to the Lyα nebula is shown in Figure 2. The Lyα nebula lies between 6 galaxies with photometric redshifts consistent with being at the nebula redshift, one of which has a grism redshift as well. In Figure 8, we show the full extent of the Lyα emission in the original Lyα imaging, within three spatial windows (10″×10″, 20″×20″, and 32″×32″). At lower surface brightnesses than shown in the discovery paper, it appears that there is a nearly complete bridge of Lyα emission between the peak of the nebula, one associated galaxy to the north, and three associated galaxies to the west (including Source 3, the source with a consistent grism redshift). At even lower surface brightnesses, the diffuse Lyα emission connects all but one of the member galaxies and traces out what appears to be two intersecting filaments, a partial ring, or an asymmetric biconical nebula roughly centered on the position of Source 6. These morphological results and the result that Source 6 is an obscured AGN plausibly at the redshift of the nebula (Section 3.1.3) are together highly suggestive that Source 6 is indeed directly associated with the presence of the Lyα nebula. Further observations, e.g., detecting CO emission lines at submillimeter wavelengths, will allow us to confirm the redshift of Source 6 and verify that we are seeing a Lyα nebula surrounding an obscured AGN.

3.3. *The Local Environment*

Thus far we have shown that there are in fact galaxies associated with the Lyα nebula. Here we assess whether the region is in fact overdense relative to the field. To be consistent with previous studies of the environments of Lyα nebulae at $z \approx 3$ (Prescott et al. 2012b), we start by plotting the number counts in the F606W band measured from within the $R < 10''$ region around the Lyα nebula and from random $R < 10''$ apertures across the full GOODS-S field (Figure 9; top panel). From this naive approach, there is only mild evidence for an enhancement in the region of the nebula; the number counts are slightly higher than in the field at $m_{F606W} \sim 25$ but consistent to within the errors, i.e., the scatter measured from the random aperture test. In addition, we have also seen from the photometric redshift analysis that there is an overdensity of $z \approx 1$ sources overlapping this region, which will necessarily boost the raw number counts. Next we look at the number density of sources with photometric redshifts within $\Delta z \pm 0.15$ of the redshift of the nebula ($z = 3.157$). In the bottom panel of Figure 9 we plot the corresponding densities for the region of the nebula and for random apertures drawn from the full GOODS-S field. The region of the nebula shows a factor of $\gtrsim$10 overdensity at $m_{F606W} \approx 25$ relative to the field galaxy population at the same photometric redshift, even when accounting for the scatter measured from randomly placed apertures. Thus, not only are there galaxies associated with the Lyα nebula, it is in fact sitting in a galaxy-overdense region of the Universe.

3.4. *Properties of the Associated Galaxies*

Having shown that Source 6 is an obscured AGN likely associated with the nebula, we briefly turn our attention to the properties of the other galaxies in this overdense region, and whether they are distinctive in any way relative to the field population. In Figure 10 we show the measured photometry and best-fit SEDs of the 6 galaxies that are likely associated with the Lyα nebula. We note that none of these member galaxies is detected in the MIPS imaging (Whitaker et al. 2014). Figure 11 shows the approximate luminosity function (LF) for the system, assuming that all 6 galaxies are at $z \approx 3.157$, as well as the ages, stellar masses, star formation rates, specific star formation rates, and A_V estimates from stellar population synthesis model fitting using FAST (Kriek et al. 2009), as reported in the 3D-HST/CANDELS catalog (Skelton et al. 2014). The galaxies are typically low luminosity, around ~ 0.2 L*, with only one (Source 3) around L*, assuming that M$^* \approx -20.8$ AB mag at this redshift (Reddy et al. 2008). The total UV luminosity of the member galaxies is $\approx$23.9 mag (AB) in the $F606W$ band, or $\approx$2.3 L*, suggesting this may be a small group in formation. The member galaxies have typical ages of around 10^8 yr, stellar masses of 10^9 M$_\odot$, star formation rates of <10 M$_\odot$ yr^{-1}, specific star formation rates of 10^{-9} yr^{-1}, and extinctions of $A_V \approx 0.2 - 0.8$ mag. In Figure 12, we show the effective radii (R_e) and Sérsic parameter (n) measurements from parametric fits to the $F160W$ imaging for the galaxies in the neighborhood of the nebula (van der Wel et al. 2012). The member galaxies are typically 1-3 kpc in radius, with Sérsic parameters clustered more around $n \approx 1$, the value for an exponential disk, than around $n \approx 4$, the value for a De Vaucouleurs profile. Two-sample Kolmogorov-Smirnov (KS) tests on all parameters did not reveal any statistical differences between the member galaxies and the field population at the same redshift ($P_{LF} = 0.17$, $P_{log(Age)} = 0.37$, $P_{log(Mass)} = 0.12$, $P_{log(SFR)} = 0.34$, $P_{log(sSFR)} = 0.92$, $P_{A_V} = 0.57$, $P_{R_e} = 0.54$, $P_n = 0.53$). This may be due to the small sample size, or it could reflect that we are witnessing an early stage in the formation of a group-mass system when the individual member galaxies are separated by large physical distances and environmental effects have yet to become important.

4. POWERING THE Lyα NEBULA

4.1. *The Energetics: Revisited*

Nilsson et al. (2006) estimated that even if Source 3, the brightest neighbor galaxy, was at the nebula redshift, it was unlikely to be able to power the Lyα emission unless highly collimated in the direction of the nebula. Extrapolating the HST B and V-band measurements of all the member galaxies, and accounting for the angle subtended by the nebula in each case, we find that galaxies can account for at most $\approx$14% of the Lyα emission, even under the optimistic assumption of an escape fraction of unity. Thus, the only source associated with the nebula that could plausibly contribute enough ionizing photons is the obscured AGN, i.e., Source 6.

The Spitzer SED of Source 6 (Figure 7) is consistent with a power-law spectrum of: $L_\nu \approx 1.7 \times 10^{30} (\nu/10^{14})^{-1.75}$ erg s^{-1} Hz^{-1}; this corresponds to a total infrared luminosity of around $\sim 1.5 \times 10^{45}$ erg s^{-1}, estimated by scaling the template of Mrk 231 to match the 8μm flux, which is approaching the realm of ultraluminous infrared galaxies (ULIRGs; $10^{12} L_\odot \approx 4 \times 10^{45}$ erg s^{-1}). Making the crude assumption that the MIR power-law can be extrapolated into the restframe UV, we estimate the ionizing photon flux of Source 6 to be $\sim 3.5 \times 10^{53}$ photons s^{-1} between restframe 200 and 912Å. Producing the observed Lyα luminosity of the nebula ($1.09 \pm 0.07 \times 10^{43}$ erg s^{-1}) requires a total of $\sim 1.0 \times 10^{54}$ photons s^{-1}, assuming that two-thirds of recombinations result in a Lyα photon. Naively, it would appear that Source 6 can only account for about 35% of the Lyα emission, even when ignoring geometrical dilution. However, this extrapolation is very uncertain; for example, a somewhat shallower power-law index of -1.5 is sufficient to match the required ionizing photon flux. If we instead take the total infrared luminosity (i.e., 3-1000μm) to be measure of the intrinsic UV/optical emission (i.e., 1000Å-1μm) that is being reprocessed by dust, we estimate that the intrisic ionizing photon flux from Source 6 is around $\sim 10^{55}$ photons s^{-1}, more than sufficient to power the nebula. Given the uncertainties about the geometry of the system, the opening angle of the AGN, the obscuration of the source, and the true SED shortward of the Lyman limit, it seems plausible that Source 6 could simply be highly obscured along our line-of-sight but less obscured in the directions of the diffuse Lyα emission. Therefore, combined with the morphological evidence in Section 3.2, it appears likely that Source 6 is responsible for a significant fraction of the ionization in the Lyα nebula.

While we have shown that there are several associated galaxies and an obscured AGN in this system that could contribute to the ionization of the nebula, we have also confirmed the previous result that there is no compact continuum source visible within the brightest part of the Lyα nebula itself. The GOODS-S HST imaging provides an upper limit on the amount of star formation that could be going on within the nebula: the 3σ limit on the $F606W$ flux (restframe ∼1400Å) of 4.66×10^{-30} that was quoted in the original paper corresponds to a limit on the UV star formation rate of $SFR(UV) = 1.4 \times 10^{-28} L_\nu < 57$ M$_\odot$ yr^{-1}, assuming the standard conversion (Kennicutt 1998). High resolution millimeter/submillimeter imaging will be important for putting further constraints on the obscured star formation and molecular gas reservoir within the nebula.

4.2. *Is the Lyα nebula gravitationally powered?*

The argument up until now has been that a Lyα nebula without any associated continuum counterparts is the best candidate for a system powered by gravitational cooling radiation. In view of our improved observational understanding of the Nilsson et al. (2006) Lyα nebula as well as updated theoretical simulations, it appears that this line of reasoning should actually be reversed, and that even this "best candidate" for a gravitationally powered Lyα nebula is in fact powered by an AGN.

A number of authors have investigated whether gravitational cooling radition within cold accretion streams can explain the observed properties of Lyα nebulae, initially with analytic arguments (Haiman et al. 2000) and then using numerical simulations (Fardal et al. 2001; Furlanetto et al. 2005; Yang et al. 2006; Dijkstra et al. 2006; Dijkstra 2009; Goerdt et al. 2010; Faucher-Giguère et al. 2010; Rosdahl & Blaizot 2012). Due to the difficulty in appropriately simulating the self-shielding of the gas and the temperature of the IGM, the maximum predicted luminosities of "cooling" Lyα nebulae from different numerical treatments have ranged from $\sim 10^{42}$ erg s^{-1}, far below that of observed samples, to $\sim 10^{44}$ erg s^{-1}, sufficient to explain even the brightest known systems. Thus it remains a matter of some debate whether gravitational cooling alone can in fact explain the large Lyα luminosities of Lyα nebulae.

At the same time, it is becoming clear that because gravitationally powered Lyα emission originates from the extended cold streams that are fueling galaxy formation, star formation, and AGN activity, the simulations generically predict that there will be a growing galaxy at the center of any luminous "cooling" Lyα nebula (e.g., Fardal et al. 2001; Furlanetto et al. 2005; Goerdt et al. 2010; Faucher-Giguère et al. 2010; Rosdahl & Blaizot 2012). Furthermore, these luminous Lyα nebulae will necessarily be hosted by $\gtrsim 10^{12}$ M$_\odot$ halos (Rosdahl & Blaizot 2012). While it is possible that such halos go through an initial phase of gas cooling preceding any substantial star formation, this cooling-only phase would necessarily have occurred much earlier, when the halo was $\sim 10^9 - 10^{10}$ M$_\odot$ and when the corresponding cooling Lyα emission was several orders of magnitude fainter than observed Lyα nebulae (Furlanetto et al. 2005). According to the most recent simulations, stellar continuum emission would therefore be expected at the position of the Lyα peak, unless this galactic counterpart has been very effectively hidden (Rosdahl & Blaizot 2012). For this reason, we suspect that the correct argument is the opposite of what has often been assumed: namely, that the lack of any associated continuum sources in the Lyα nebula makes it *less likely* that this system is predominantly powered by gravitational cooling. It is difficult to understand how the central growing galaxy, presumably the most massive member in the region located at a node within the cosmic web, has been so effectively hidden at the center of the Lyα nebula. If it is simply highly obscured and therefore not visible in the restframe optical, then it should be the brightest source visible in the system at longer wavelengths. Higher resolution millimeter/submillimeter observations will be important for shedding further light on this issue, but the evidence thus far from the Spitzer data is that the bulk of the obscured emission in this system is concentrated at the position of Source 6, an obscured AGN that is offset by $\sim 4'' \approx 30$ kpc from the brightest part of the Lyα nebula and that is instead located in an apparent "hole" in the fainter, larger scale Lyα emission. Thus, while it is still possible that the Lyα emission is tracing gas within cosmic filaments, the results of this paper argue strongly that it is being powered primarily by illumination from the obscured AGN in the region instead of by gravitational cooling.

We suspect that this Lyα nebula is not an isolated case. The key observational characteristics of this system - the small sizes, disk-like morphologies, and low luminosities of the member galaxies, the evidence for an overdense neighborhood, and the presence of a highly obscured AGN offset by 10s of kpc from the Lyα peak that can provide some if not all of the requisite ionizing photons - are highly reminiscent of the properties LABd05, a more luminous Lyα nebula at $z \approx 2.7$ (Prescott et al. 2012b). It seems likely that these systems are intrinsically similar to cases such as Weidinger et al. (2004, 2005), a quasar at $z \approx 3$ with an extended, asymmetric biconical Lyα halo that is being viewed through one side of the ionization cone of the (unobscured) quasar. In the Nilsson et al. (2006) Lyα nebula, we are likely observing a similar phenomenon, an AGN powering an extended Lyα nebula, but with a line-of-sight passing outside the ionization cone. This picture is broadly consistent with the much higher obscuration of the AGN and the two lobe structure seen at low surface brightness levels in the Lyα emission. Our conclusions are consistent with the argument of Overzier et al. (2013) that AGN must be the dominant power source for the majority (if not all) of the most luminous Lyα nebulae. The Nilsson et al. (2006) Lya nebula is somewhat lower luminosity than the systems studied by Overzier et al. (2013), suggesting that even at lower luminosities where less powerful mechanisms (gravitational cooling, winds, star formation) could in principle play a larger role, AGN continue to be a dominant power source for Lyα nebulae.

5. IMPLICATIONS

On a more general level, while gravitational cooling radiation, as a fundamental physical process, must contribute to the total Lyα emission observed from Lyα nebulae, our experience with this Lyα nebula leads us to conclude that it will always be more difficult to prove that a given nebula is primarily gravitationally powered. Since bright Lyα emission from gravitationally cooling correlates strongly with actively growing galaxies (and AGN), a lack of obvious power sources is not sufficient evidence, and the morphology and shape of the surface brightness profile could simply reflect the fact that the gas is being brought in by a cold accretion stream without necessarily proving the nebula is lit up by gravitational cooling. Determining what fraction of a given Lyα nebula is powered by gravity as opposed to by embedded sources requires more detailed studies of, e.g., the polarization of the Lyα emission to constrain the contribution of scattered light, as well as comparisons between emission line diagnostic measurements within the diffuse gas and improved theoretical predictions for the expected metal line emission from cold accrection streams.

Instead, we suspect that extended Lyα emission displaced from all associated continuum sources is actually *less likely* to be powered by cooling radition and *more likely* to be a signature of cosmic gas illuminated by an offset AGN (leading to either Lyα fluorescence or Lyα resonant scattering), an AGN that may be highly-obscured to the line-of-sight or recently extinguished. It is not particularly hard to hide an AGN with obscuration and geometry (i.e., if it is offset from the nebula and obscured to our line-of-sight but unobscured towards the nebula), or if it is in the process of ramping down in its output, leaving a seemingly-abandoned light echo of Lyα emission at larger distances (and light travel times) from the AGN position (e.g., similar to Hanny's Voorwerp, an [O III] nebula at lower redshift; Schawinski et al. 2010). In systems where we can identify an AGN as the dominant power source in this way, we have an opportunity to use the spatially extended line emission as a laboratory for studying AGN variability over 10^4-10^5 year timescales as well as the physical conditions within the underlying cosmic web, lit up in emission while in the process of fueling and being impacted by ongoing local galaxy formation.

6. CONCLUSIONS

In light of new observations and more sophisticated numerical simulations, we have taken a second look at the local environment and most likely power source for the Nilsson et al. (2006) Lyα nebula. We find that the nebula is associated with 6 nearby galaxies and an obscured AGN located $\sim 4'' \approx 30$ kpc away. The Lyα emission is seen to extend further than previously realized, nearly encircling the position of the obscured AGN, and the local region shows evidence for being overdense relative to the field. At the same time, results from the latest generation of cold accretion simulations show that the brightest Lyα emission powered by gravitational cooling will be centered on a growing galaxy, which should be detectable as a counterpart in the continuum. Thus, while we confirm the previous finding that there is no associated continuum source located within the nebula itself, we conclude that this is actually a strong argument *against*, rather than for, the nebula being powered by gravitational energy. The Lyα emission at low surface brightness levels appears to trace out a complicated filamentary structure, perhaps consistent with gas within cold accretion streams, but this gas is most plausibly being lit up due to illumination from a nearby obscured AGN rather than due to gravitational powering. Follow-up observations of such emission line nebulae offer an exciting window into both AGN physics and the kinematics and physical conditions of the cosmic web surrounding regions of active galaxy formation.

We are grateful to Kim Nilsson for assistance with the original Lyα data, to Rosalind Skelton for guidance on using the 3D-HST/CANDELS photometric catalog, to Julie Wardlow and the HerMES team for providing early access to the HerMES catalogs, and to Lise Christensen, Kristian Finlator, Sebastian Hönig, Pieter van Dokkum, Natascha Förster Schreiber, and the anonymous referee for helpful discussions and comments.

M.K.M.P. was supported by a Dark Cosmology Centre Fellowship. J.P.U.F. acknowledges support from the ERC-StG grant EGGS-278202. The Dark Cosmology Centre is funded by The Danish National Research Foundation.

This work is based on observations taken by the WFC3 Early Release Science program (GO 11359 and 11360) and the 3D-HST Treasury Program (GO 12177 and 12328) with the NASA/ESA HST, which is operated by the Association of Universities for Research in Astronomy, Inc., under NASA contract NAS5-26555.

The GOODS-Herschel data was accessed through the Herschel Database in Marseille (HeDaM - http://hedam.lam.fr) operated by CeSAM and hosted by the Laboratoire d'Astrophysique de Marseille.

This research has made use of data from HerMES project (http://hermes.sussex.ac.uk/). HerMES is a Herschel Key Programme utilising Guaranteed Time from the SPIRE instrument team, ESAC scientists and a mission scientist.

REFERENCES

Adams, J. J., Hill, G. J., & MacQueen, P. J. 2009, The Astrophysical Journal, 694, 314

Brammer, G. B., van Dokkum, P. G., & Coppi, P. 2008, The Astrophysical Journal, 686, 1503

Cantalupo, S., Porciani, C., Lilly, S. J., & Miniati, F. 2005, The Astrophysical Journal, 628, 61

Cen, R., & Zheng, Z. 2013, The Astrophysical Journal, 775, 112

Colbert, J. W., Scarlata, C., Teplitz, H., Francis, P., Palunas, P., Williger, G. M., & Woodgate, B. 2011, The Astrophysical Journal, 728, 59

Dahlen, T., et al. 2013, The Astrophysical Journal, 775, 93

Dekel, A., et al. 2009, Nature, 457, 451

Dickinson, M., et al. 2004, The Astrophysical Journal, 600, L99

Dijkstra, M. 2009, The Astrophysical Journal, 690, 82

Dijkstra, M., Haiman, Z., & Spaans, M. 2006, The Astrophysical Journal, 649, 14

Donley, J. L., Rieke, G. H., Pérez-González, P. G., & Barro, G. 2008, The Astrophysical Journal, 687, 111

Donley, J. L., Rieke, G. H., PerezGonzalez, P. G., Rigby, J. R., & AlonsoHerrero, A. 2007, The Astrophysical Journal, 660, 167

Donley, J. L., et al. 2012, The Astrophysical Journal, 748, 142

Elbaz, D., et al. 2011, Astronomy & Astrophysics, 533, A119

Erb, D. K., Bogosavljević, M., & Steidel, C. C. 2011, The Astrophysical Journal, 740, L31

Fardal, M. A., Katz, N., Gardner, J. P., Hernquist, L., Weinberg, D. H., & Dave, R. 2001, The Astrophysical Journal, 562, 605

Faucher-Giguère, C.-A., Kereš, D., Dijkstra, M., Hernquist, L., & Zaldarriaga, M. 2010, The Astrophysical Journal, 725, 633

Furlanetto, S. R., Schaye, J., Springel, V., & Hernquist, L. 2005, The Astrophysical Journal, 622, 7

Geach, J. E., et al. 2009, The Astrophysical Journal, 700, 1

Giavalisco, M., et al. 2004, The Astrophysical Journal, 600, L93

Goerdt, T., Dekel, A., Sternberg, A., Ceverino, D., Teyssier, R., & Primack, J. R. 2010, Monthly Notices of the Royal Astronomical Society, 407, 613

Haiman, Z., Spaans, M., & Quataert, E. 2000, The Astrophysical Journal, 537, L5

Hayes, M., Scarlata, C., & Siana, B. 2011, Nature, 476, 304

Ivison, R. J., et al. 2004, The Astrophysical Journal Supplement Series, 154, 124

Kennicutt, R. C. 1998, The Astrophysical Journal, 498, 541

Keres, D., Katz, N., Weinberg, D. H., & Dave, R. 2005, Monthly Notices of the Royal Astronomical Society, 363, 2

Kollmeier, J. A., Zheng, Z., Davé, R., Gould, A., Katz, N., Miralda-Escudé, J., & Weinberg, D. H. 2010, The Astrophysical Journal, 708, 1048

Kriek, M., van Dokkum, P. G., Labbé, I., Franx, M., Illingworth, G. D., Marchesini, D., & Quadri, R. F. 2009, The Astrophysical Journal, 700, 221

Lacy, M., Petric, A. O., Sajina, A., Canalizo, G., Storrie-Lombardi, L. J., Armus, L., Fadda, D., & Marleau, F. R. 2007, The Astronomical Journal, 133, 186

Lacy, M., et al. 2004, The Astrophysical Journal Supplement Series, 154, 166

Laursen, P., Duval, F., & Östlin, G. 2013, The Astrophysical Journal, 766, 124

Laursen, P., & Sommer-Larsen, J. 2007, The Astrophysical Journal, 657, L69

Laursen, P., Sommer-Larsen, J., & Andersen, A. C. 2009, The Astrophysical Journal, 704, 1640

Levenson, L., et al. 2010, Monthly Notices of the Royal Astronomical Society, 409, 83

Luo, B., et al. 2008, The Astrophysical Journal Supplement Series, 179, 19

Møller, P., & Warren, S. J. 1998, Monthly Notices of the Royal Astronomical Society, 299, 661

Mori, M., Umemura, M., & Ferrara, A. 2004, The Astrophysical Journal, 613, L97

Nilsson, K. K., Fynbo, J. P. U., Møller, P., Sommer-Larsen, J., & Ledoux, C. 2006, Astronomy and Astrophysics, 452, L23

Nilsson, K. K., et al. 2007, Astronomy and Astrophysics, 471, 71

Oke, J. B. 1974, The Astrophysical Journal Supplement Series, 27, 21

Oliver, S. J., et al. 2012, Monthly Notices of the Royal Astronomical Society, 424, 1614

Overzier, R. A., Nesvadba, N. P. H., Dijkstra, M., Hatch, N. A., Lehnert, M. D., Villar-Martín, M., Wilman, R. J., & Zirm, A. W. 2013, The Astrophysical Journal, 771, 89

Polletta, M., et al. 2007, The Astrophysical Journal, 663, 81

Prescott, M. K. M., Dey, A., & Jannuzi, B. T. 2009, The Astrophysical Journal, 702, 554

Prescott, M. K. M., Dey, A., & Jannuzi, B. T. 2012a, The Astrophysical Journal, 748, 125

Prescott, M. K. M., Dey, A., & Jannuzi, B. T. 2013, The Astrophysical Journal, 762, 38

Prescott, M. K. M., et al. 2012b, The Astrophysical Journal, 752, 86

Rasmussen, J., Sommer-Larsen, J., Pedersen, K., Toft, S., Benson, A., Bower, R. G., & Grove, L. F. 2009, The Astrophysical Journal, 697, 79

Reddy, N. A., Steidel, C. C., Pettini, M., Adelberger, K. L., Shapley, A. E., Erb, D. K., & Dickinson, M. 2008, The Astrophysical Journal Supplement Series, 175, 48

Rosdahl, J., & Blaizot, J. 2012, Monthly Notices of the Royal Astronomical Society, 423, 344

Roseboom, I. G., et al. 2010, Monthly Notices of the Royal Astronomical Society, 409, 48

Roseboom, I. G., et al. 2012, Monthly Notices of the Royal Astronomical Society, 419, 2758

Schawinski, K., et al. 2010, The Astrophysical Journal, 724, L30

Skelton, R. E., et al. 2014, The Astrophysical Journal Supplement Series, 214, 24

Smith, D. J. B., Jarvis, M. J., Lacy, M., & Martínez-Sansigre, A. 2008, Monthly Notices of the Royal Astronomical Society, 389, 799

Steidel, C. C., Bogosavljević, M., Shapley, A. E., Kollmeier, J. A., Reddy, N. A., Erb, D. K., & Pettini, M. 2011, The Astrophysical Journal, 736, 160

Stern, D., et al. 2005, The Astrophysical Journal, 631, 163

Tamura, Y., et al. 2013, Monthly Notices of the Royal Astronomical Society, 430, 2768

Taniguchi, Y., & Shioya, Y. 2000, The Astrophysical Journal, 532, L13

Taniguchi, Y., Shioya, Y., & Kakazu, Y. 2001, The Astrophysical Journal, 562, L15

van der Wel, A., et al. 2012, The Astrophysical Journal Supplement Series, 203, 24

Weidinger, M., Møller, P., & Fynbo, J. P. U. 2004, Nature, 430, 999

Weidinger, M., Møller, P., Fynbo, J. P. U., & Thomsen, B. 2005, Astronomy and Astrophysics, 436, 825

Weijmans, A.-M., Bower, R. G., Geach, J. E., Swinbank, A. M., Wilman, R. J., de Zeeuw, P. T., & Morris, S. L. 2010, Monthly Notices of the Royal Astronomical Society, 402, 2245

Whitaker, K. E., et al. 2014, The Astrophysical Journal, 795, 104

Windhorst, R. A., et al. 2011, The Astrophysical Journal Supplement Series, 193, 27

Xue, Y. Q., et al. 2011, The Astrophysical Journal Supplement Series, 195, 10

Yajima, H., Li, Y., & Zhu, Q. 2013, The Astrophysical Journal, 773, 151

Yang, Y., Walter, F., Decarli, R., Bertoldi, F., Weiss, A., Dey, A., Prescott, M. K. M., & Bdescu, T. 2014, The Astrophysical Journal, 784, 171

Yang, Y., Zabludoff, A., Eisenstein, D., & Davé, R. 2010, The Astrophysical Journal, 719, 1654

Yang, Y., Zabludoff, A. I., Dave, R., Eisenstein, D. J., Pinto, P. A., Katz, N., Weinberg, D. H., & Barton, E. J. 2006, The Astrophysical Journal, 640, 539

Zheng, Z., Cen, R., Weinberg, D., Trac, H., & Miralda-Escudé, J. 2011, The Astrophysical Journal, 739, 62

Table 1
Likely Galaxy Members

ID[a]	3D-HST/CANDELS Catalog ID	Right Ascension (hours)	Declination (degrees)	m_{F160W}	z_{phot}	z_{grism}	Notes
3	GOODS-S-41192	03:32:14.072	-27:43:03.72	23.54	$3.206^{+0.065}_{-0.058}$	$3.153^{+0.019}_{-0.004}$	
8	GOODS-S-41189	03:32:14.886	-27:43:03.54	24.83	$3.246^{+0.104}_{-0.101}$	-	
9	GOODS-S-41027	03:32:14.070	-27:43:05.27	26.06	$3.179^{+0.160}_{-0.171}$	-	
10	GOODS-S-41047	03:32:13.947	-27:43:04.81	26.02	$3.204^{+0.308}_{-0.293}$	-	
11	GOODS-S-41395	03:32:14.550	-27:42:59.34	25.36	$3.036^{+0.085}_{-0.085}$	-	
12	GOODS-S-41673	03:32:14.884	-27:42:54.27	27.26	$3.231^{+0.188}_{-0.212}$	-	
6		03:32:14.606	-27:43:06.14		$3.801^{+1.786}_{-0.513}$	-	IRAC data / SF templates only included in the photometric redshift fit
					$3.094^{+2.097}_{-0.272}$	-	IRAC and MIPS data / AGN and SF templates included in photometric redshift fit

[a] The ID column is based on the numbering scheme used in Nilsson et al. (2006).

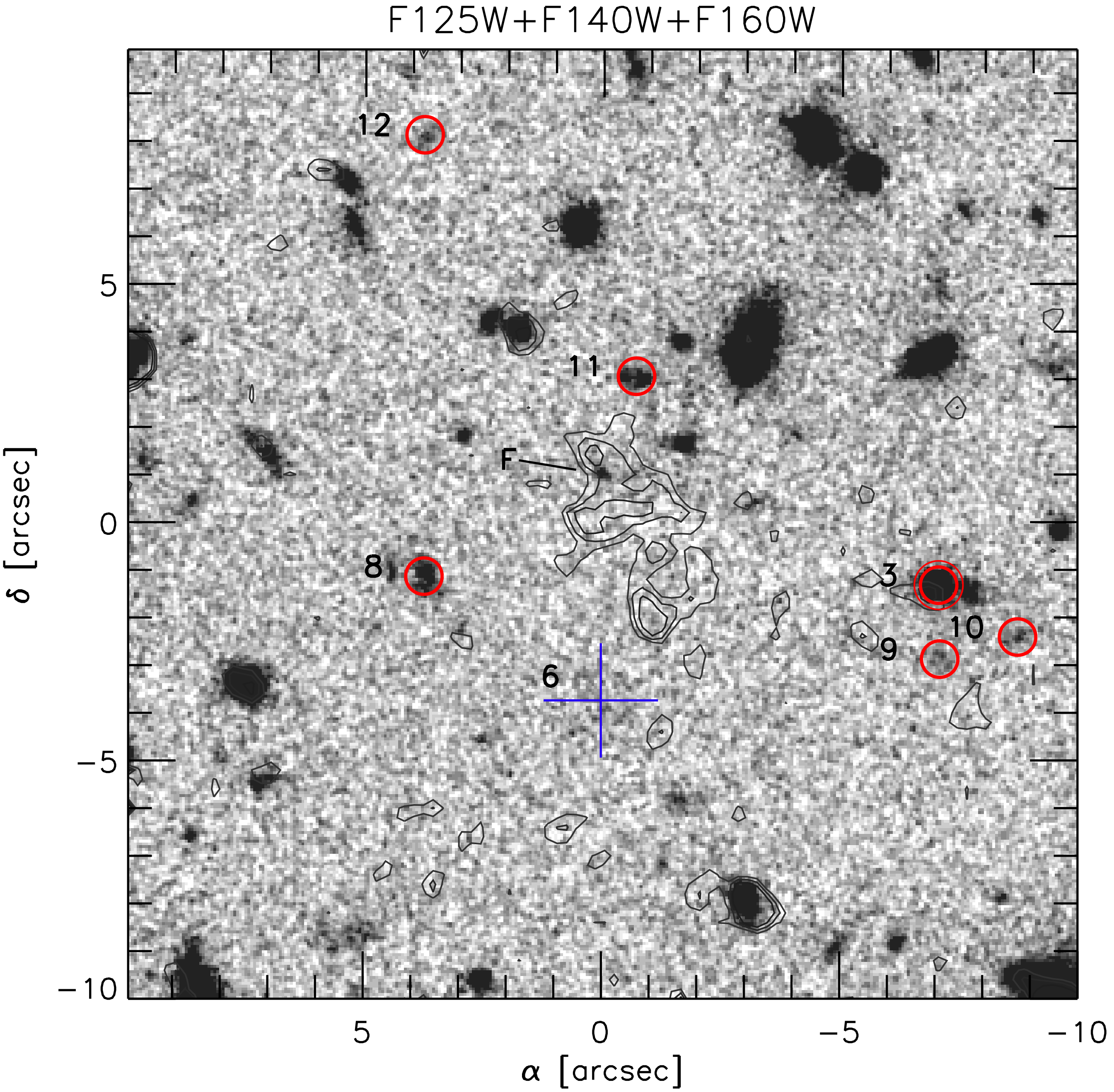

Figure 1. Stacked WFC3-IR/*F125W*, *F140W*, and *F160W* imaging of the region around the Lyα nebula. The Lyα emission is shown with black contours at Lyα surface brightness levels of $[5.3,7.0,8.9]\times10^{-18}$ erg s^{-1} cm^{-2} arcsec^{-2} after smoothing by $0.4 \times 0.4''$. Sources with photometric redshifts within $\Delta z = 0.15$ are shown (red circles), while Source 3, the galaxy with a consistent grism redshift, is indicated with a double red circle. The IRAC centroid of Source 6 from the GOODS-Herschel catalog is indicated with a blue cross. The galaxy located closest to the Lyα peak, labeled 'F', is a foreground galaxy at $z \approx 1$.

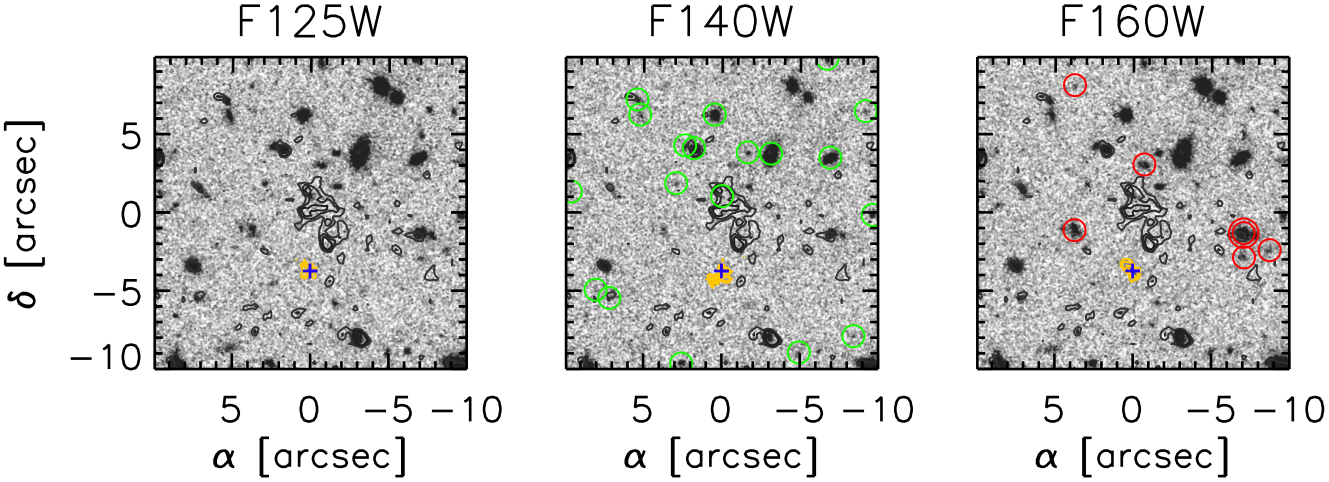

Figure 2. Region around the Lyα nebula in the individual WFC3-IR/$F125W$, $F140W$, and $F160W$ images. In all panels the Lyα nebula is shown with black contours at Lyα surface brightness levels of $[5.3,7.0,8.9]\times10^{-18}$ erg s^{-1} cm^{-2} arcsec^{-2} after smoothing by $0.4\times0.4''$. The IRAC centroid of Source 6 from the GOODS-Herschel catalog is indicated with a blue cross, and the yellow contours in each panel highlight diffuse emission in the corresponding WFC3-IR image that is detected within $R<1.3''$ of Source 6. **Left:** The WFC3 $F125W$ image. The $F125W$ surface brightness contours at the position of Source 6 (yellow lines) correspond to $SB_{F125W}=[0.4,0.6,0.8]\times10^{-20}$ erg s^{-1} cm^{-2} Å^{-1} arcsec^{-2}. **Middle:** The WFC3 $F140W$ image; foreground sources with photometric redshifts within $\Delta z\pm0.15$ of $z=1$ are indicated (green circles). The $F140W$ surface brightness contours at the position of Source 6 (yellow lines) correspond to $SB_{F140W}=[0.8,1.0,1.2]\times10^{-20}$ erg s^{-1} cm^{-2} Å^{-1} arcsec^{-2}. **Right:** The WFC3 $F160W$ image; sources with photometric redshifts within $\Delta z\pm0.15$ of the redshift of the Lyα nebula are indicated (red circles). The source with a detection of [OII] at $z=3.153$ in the $G141$ grism data is shown with a larger red circle. The $F160W$ surface brightness contours at the position of Source 6 (yellow lines) correspond to $SB_{F160W}=[0.8,1.0,1.2]\times10^{-20}$ erg s^{-1} cm^{-2} Å^{-1} arcsec^{-2}.

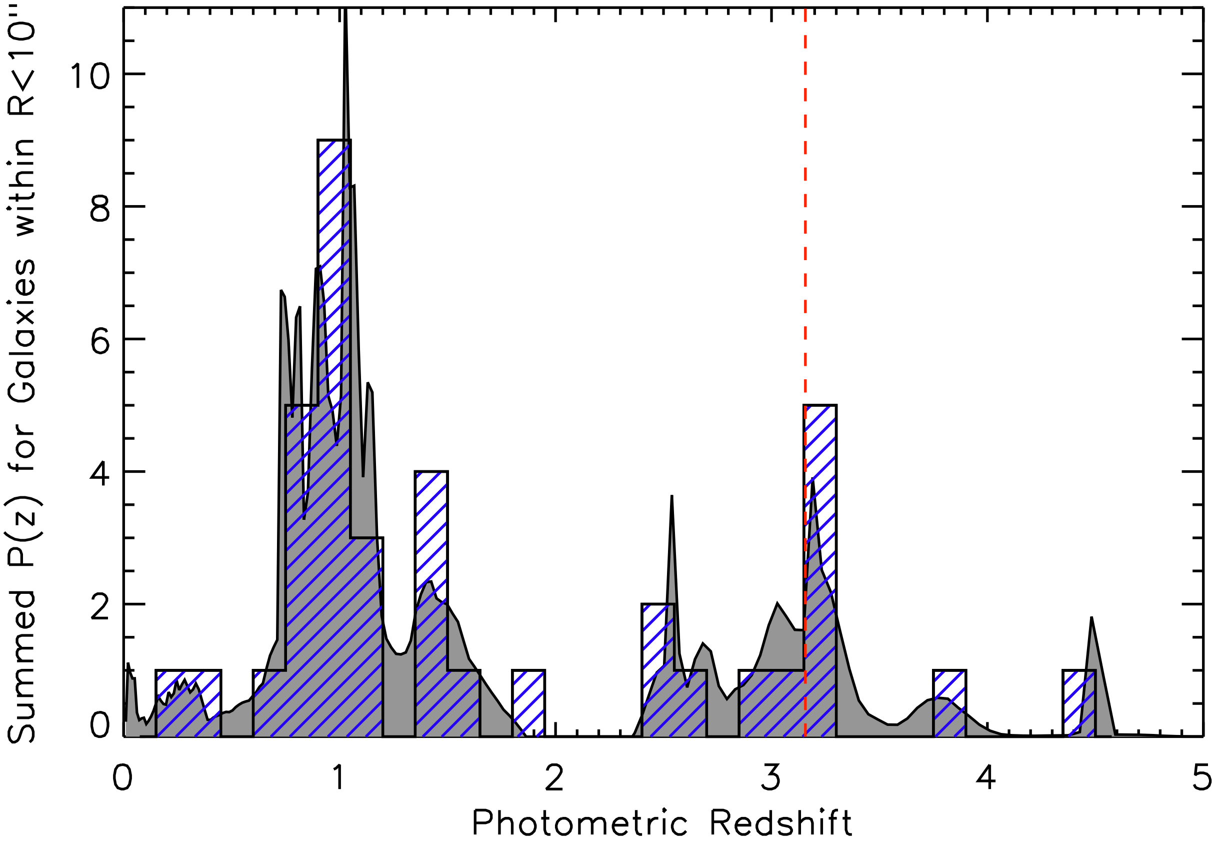

Figure 3. Photometric redshift distribution for sources within $R < 10''$ of the Lyα nebula. The summed P(z) distribution is shown (grey shading) along with a histogram of the best fit photometric redshifts (blue hashed histogram). The redshift of the Lyα nebula is indicated with the red dashed line.

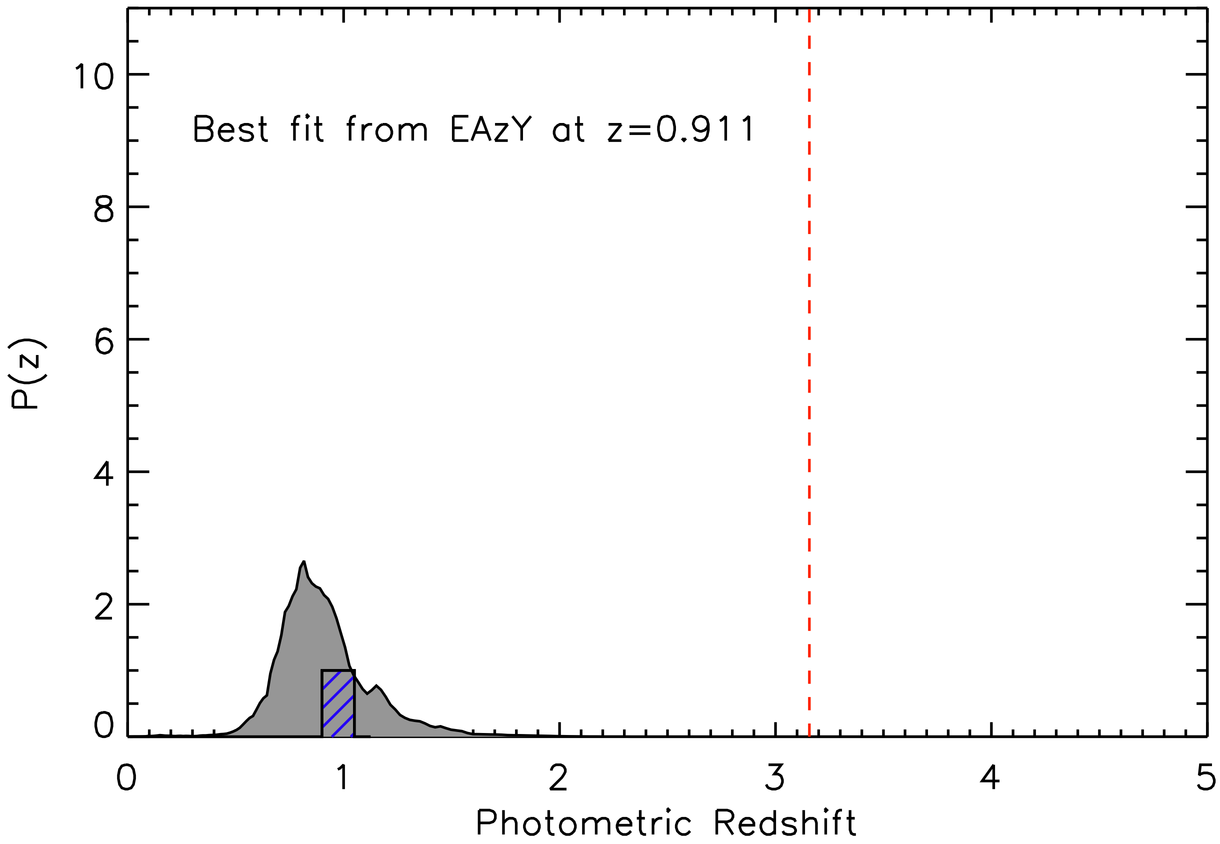

Figure 4. Photometric redshift distribution for Galaxy 'F', the faint galaxy closest to the peak of the Lyα emission. The P(z) distribution is shown (grey shading) along with a histogram showing the best fit photometric redshift (blue hashed). The redshift of the Lyα nebula is indicated with the red dashed line.

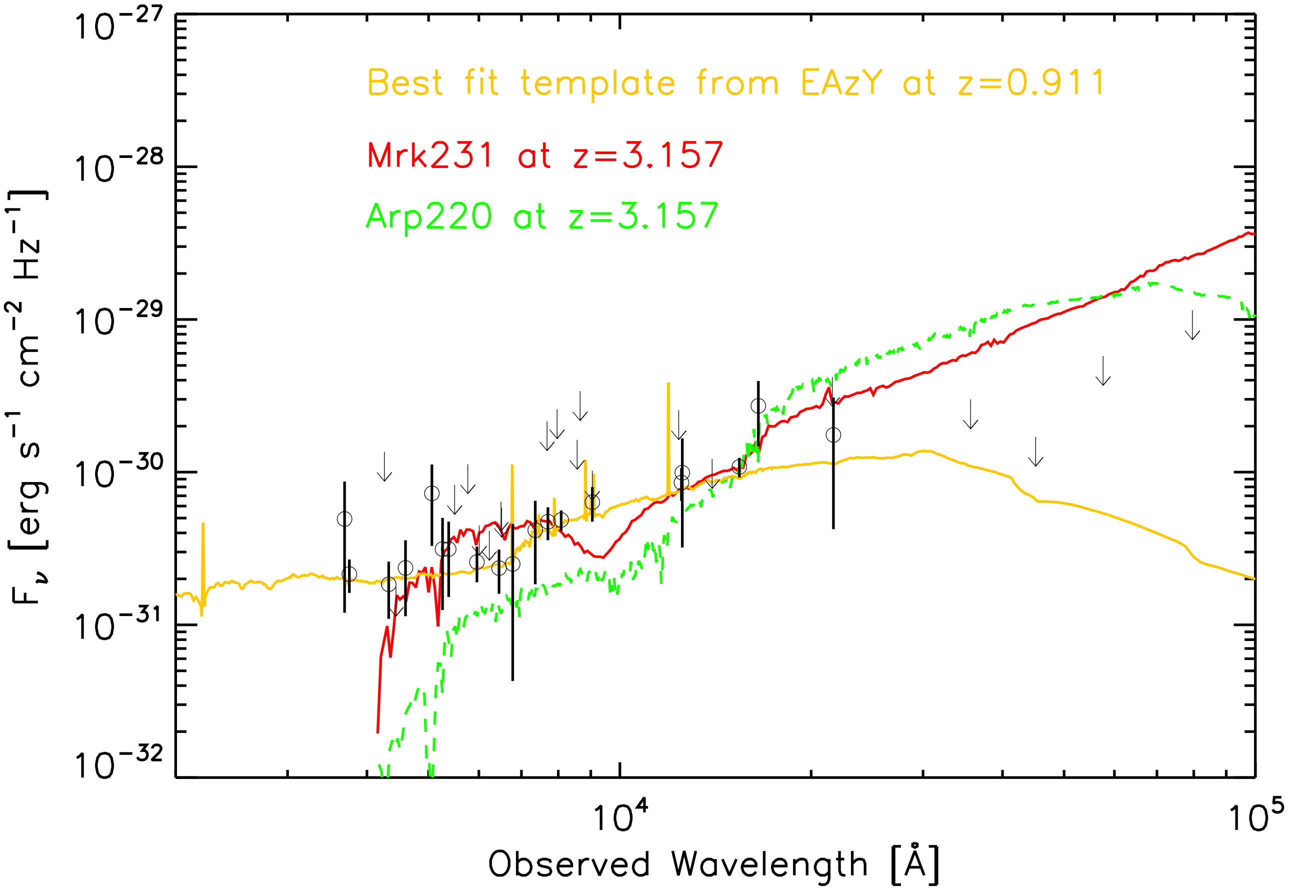

Figure 5. SED (open black circles and arrows representing 3σ upper limits) and best-fit EAzY template (yellow solid line) for Galaxy 'F', the faint source closest to the peak of the Lyα emission, as compared with Mrk231 (red solid line) and Arp220 (green dashed line) templates shifted to $z = 3.157$. Despite being located very near the Lyα peak, this source is inconsistent with being at the nebula redshift. It is instead part of the overdensity of $z \approx 1$ sources that overlaps this location.

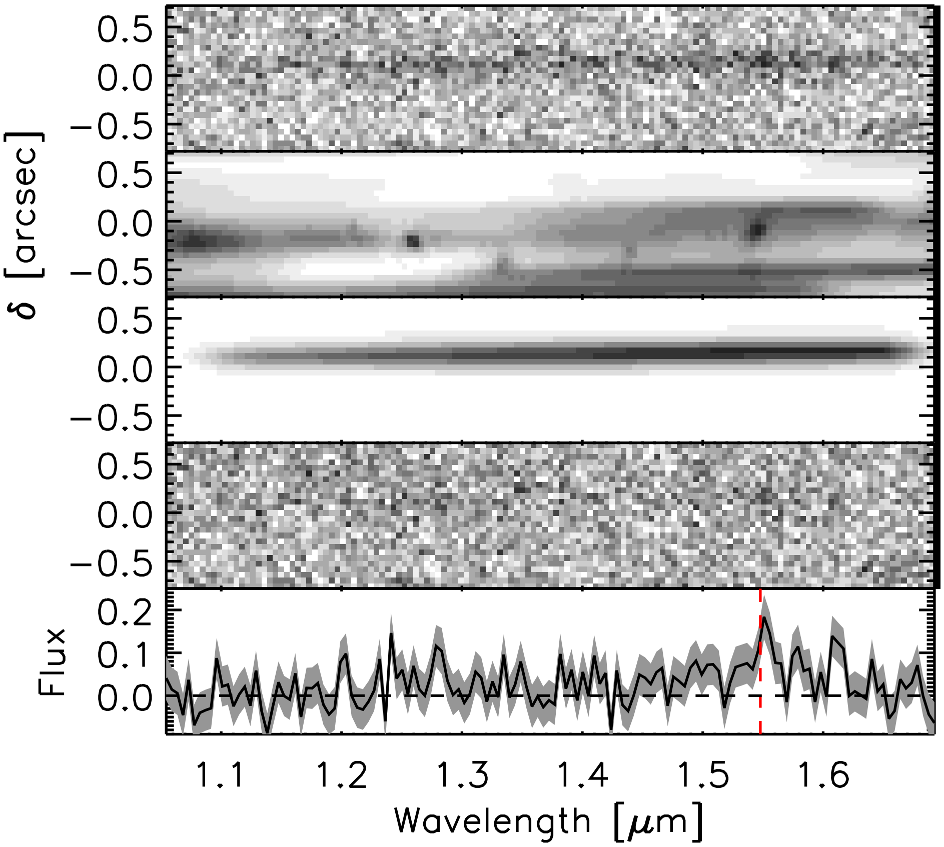

Figure 6. Grism spectroscopy of Source 3, showing the 2D grism spectrum (top row), the contamination model corresponding to flux from nearby sources (second row), the continuum model (third row), the continuum- and contamination-subtracted grism spectrum (fourth row), and the 1D spectral extraction (bottom row) with the corresponding errors overplotted (grey shading) and the position of the measured [OII] line indicated (vertical dashed red line).

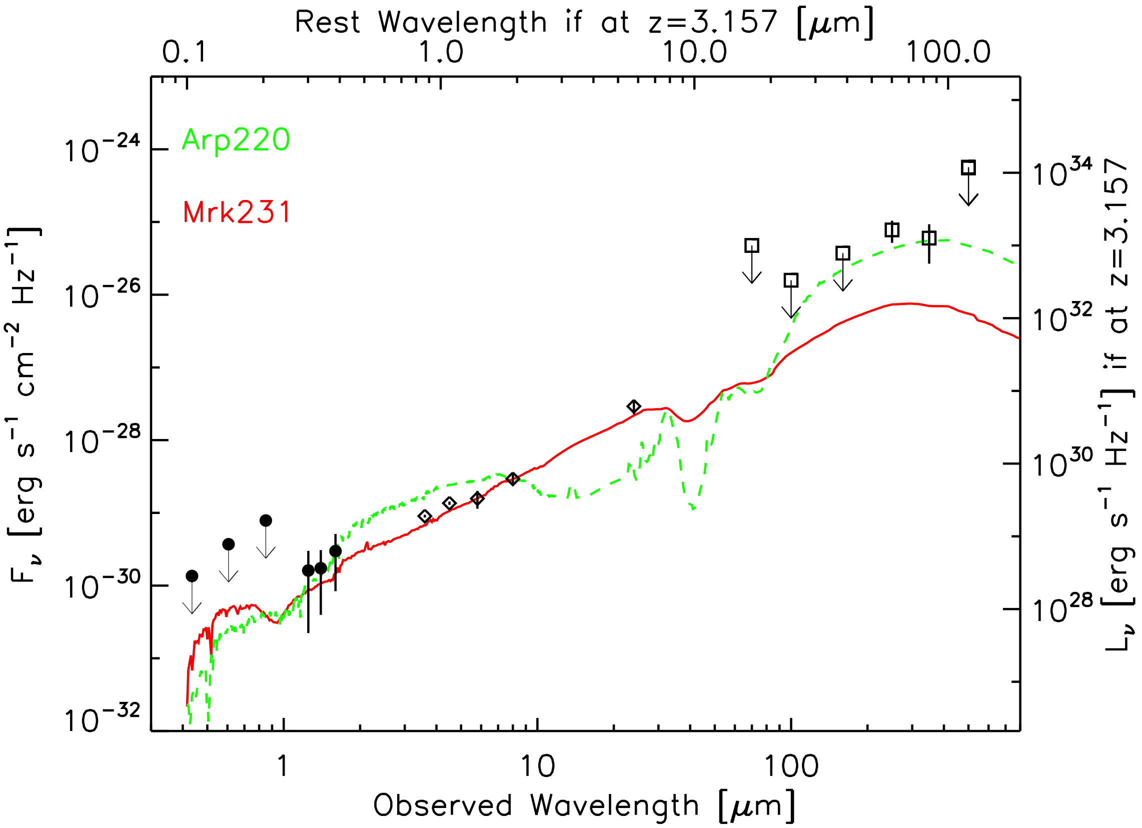

Figure 7. Source 6 SED from HST (filled circles), Spitzer (open diamonds), and Herschel (open squares). All upper limits are shown at 3σ. Mrk231 (red solid line) and Arp220 (green dashed line) templates are shown for reference (Polletta et al. 2007), scaled to the 8μm data point. The top axis gives the corresponding rest wavelength and the right axis the corresponding luminosity density L_ν, assuming Source 6 is at the redshift of the Lyα nebula. The mid-infrared data are much better fit by the Mrk231 (AGN) template; the Herschel detections may be contaminated by source confusion, but suggest there may be an additional cool dust component.

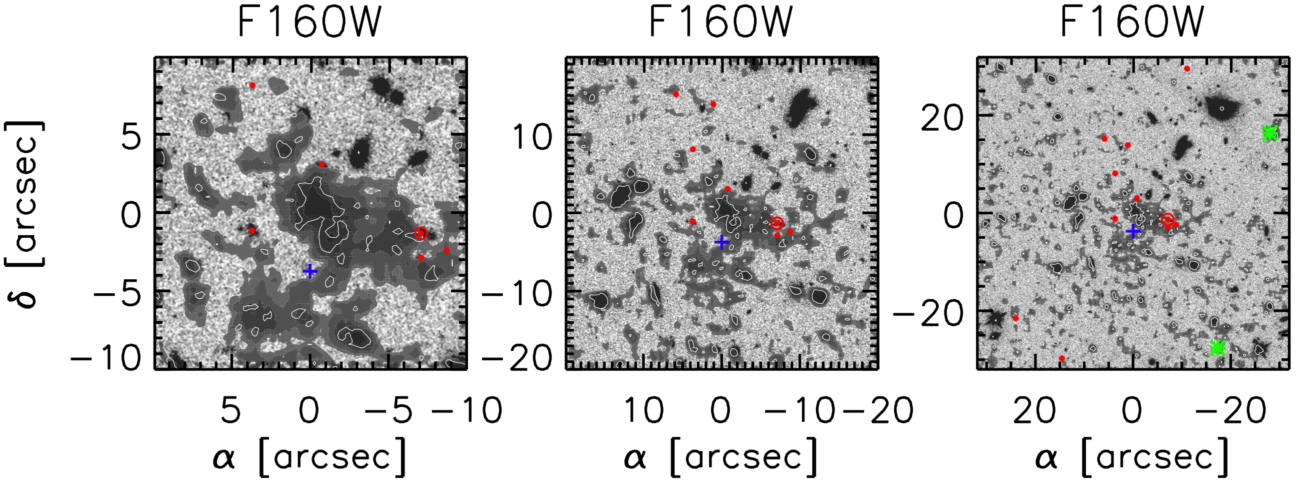

Figure 8. Spatial extent of the Lyα emission overplotted on the *F160W* imaging. In all panels the Lyα nebula, as shown in previous figures, is outlined with white contours (corresponding to a surface brightness level of 5.3×10^{-18} erg s^{-1} cm^{-2} arcsec^{-2}), while additional Lyα surface brightness contours are shown in greyscale at $[1.3,1.9,3.2,4.4,6.3]\times10^{-18}$ erg s^{-1} cm^{-2} arcsec^{-2} after smoothing by $0.4\times0.4''$. Sources with photometric redshifts within $\Delta z \pm 0.15$ of the redshift of the Lyα nebula are highlighted with red points, and Source 3, the source with a weak [OII] detection at $z = 3.153$ in the $G141$ grism data, is shown with a larger red circle. The position of Source 6 is indicated with a blue cross. LAEs from Nilsson et al. (2007) are shown as green stars.

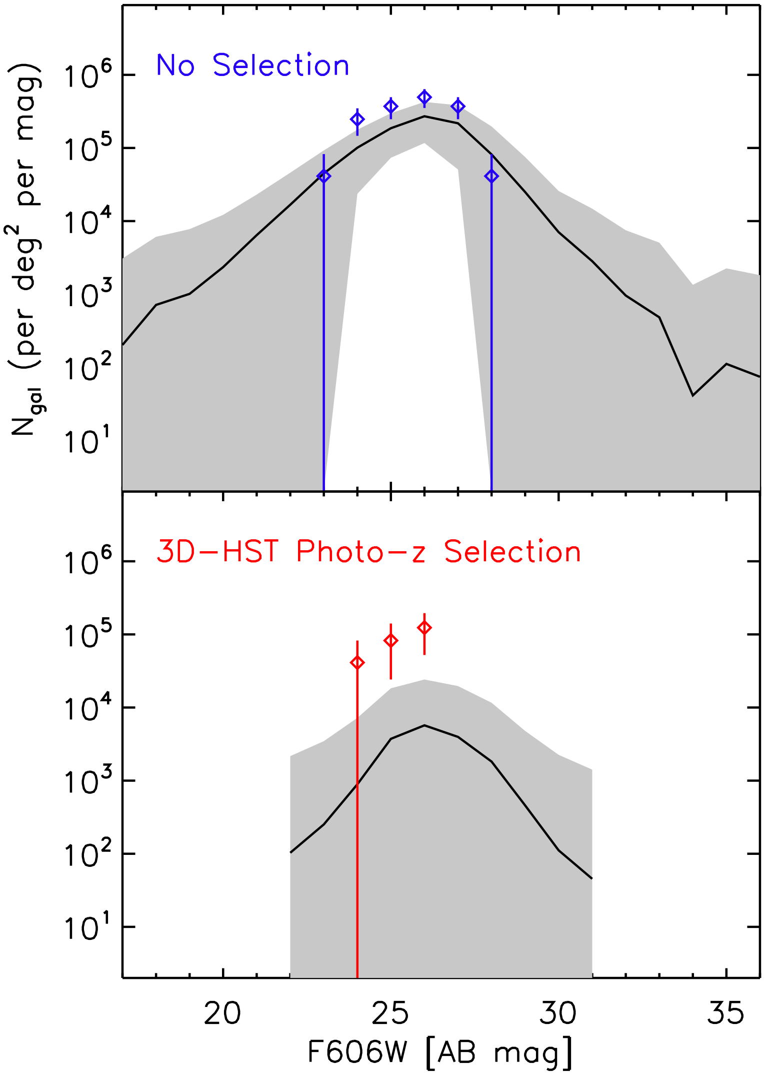

Figure 9. **Top:** Number counts in the $F606W$ band measured from the region around the Lyα nebula ($R < 10''$; blue diamonds) and from within random $R < 10''$ apertures across the entire GOODS-S field (with the mean and standard deviation shown as the black line and grey region, respectively). The $F606W$ band was chosen to be consistent with previous studies of the environments of Lyα nebulae at $z \approx 3$ (Prescott et al. 2012b). **Bottom:** Sources with photometric redshifts within $\Delta z \pm 0.15$ of the Lyα nebula redshift measured from the region around the Lyα nebula ($R < 10''$; red diamonds) and from within random $R < 10''$ apertures across the entire GOODS-S field (with the mean and standard deviation shown as the black line and grey region, respectively).

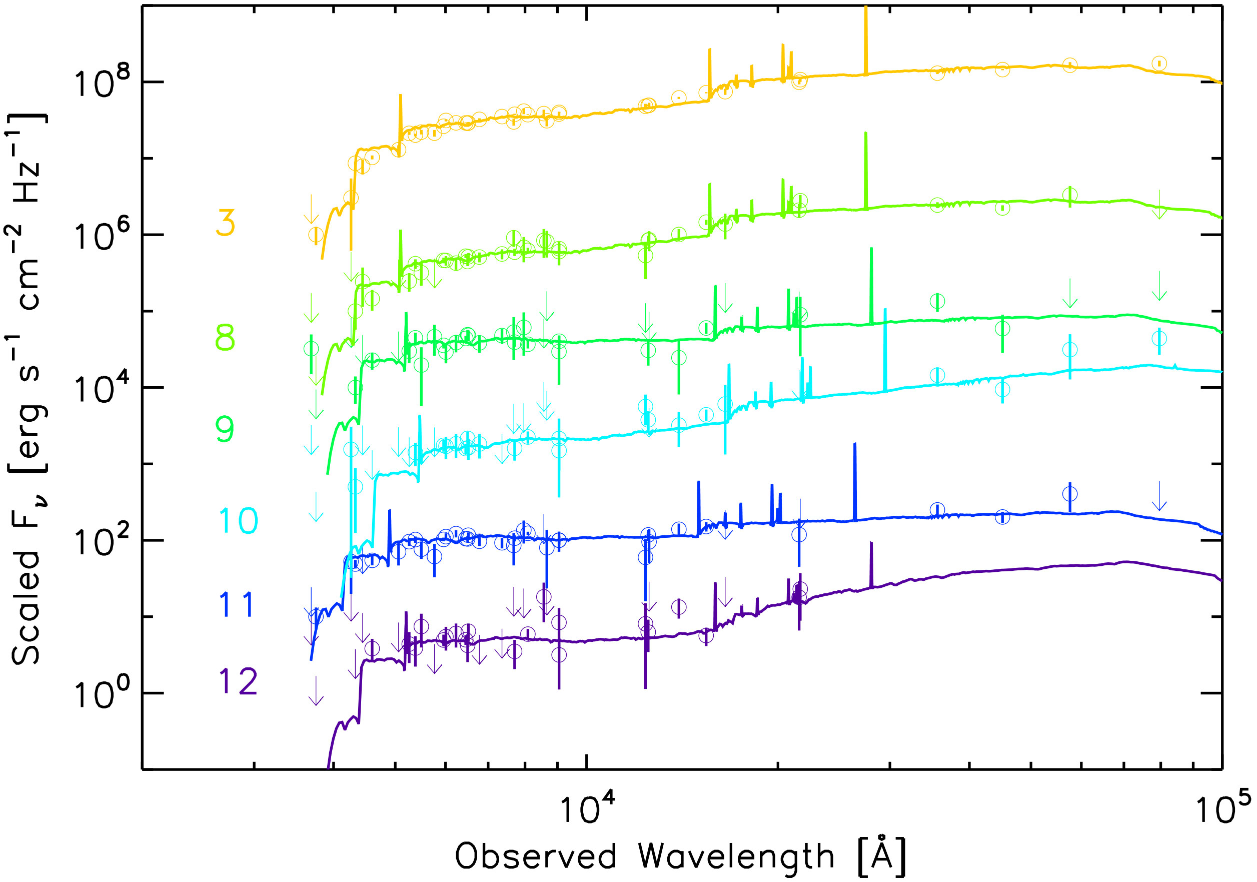

Figure 10. Photometry and best-fit EAzY SEDs (open circles and arrows representing 3σ upper limits) of the 6 galaxies likely associated with the Lyα nebula (Skelton et al. 2014). Numbers correspond to the source IDs in Table 1.

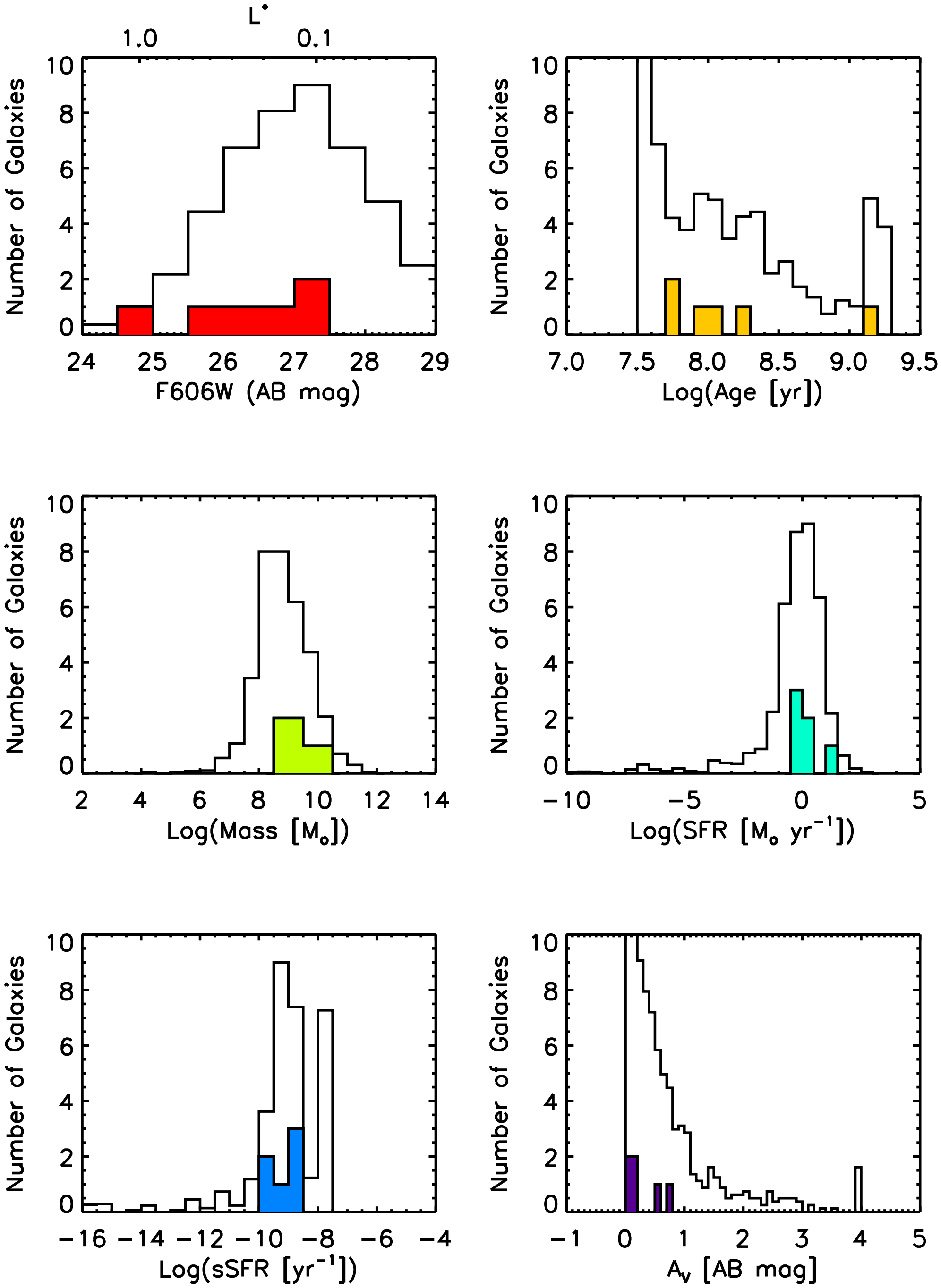

Figure 11. Luminosity function and physical properties derived from SED fitting (Skelton et al. 2014) for galaxies associated with the Lyα nebula (filled histograms) versus all galaxies in the field within $\Delta z \pm 0.15$ (open histograms, scaled down for clarity). **Top Left:** $F606W$-band luminosity function (AB mag). **Top Right:** Log of the stellar age in years. **Middle Left:** Log of the stellar mass in solar masses. **Middle Right:** Log of the star formation rate in solar masses per year. **Bottom Left:** Log of the specific star formation rate in inverse years. **Bottom Right:** Attenuation A_V (AB mag).

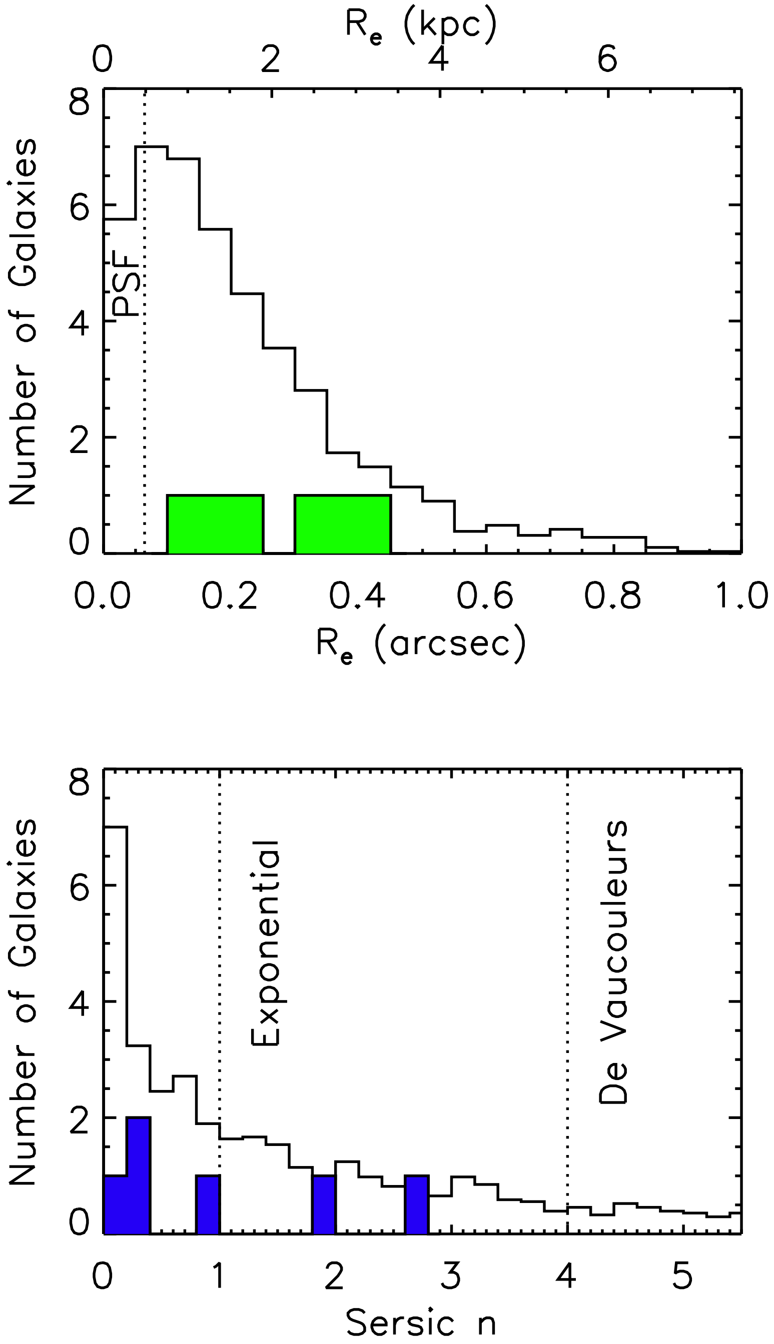

Figure 12. Effective radius (R_e) and Sérsic n estimates derived from GALFIT parametric fits to the $F160W$ data (van der Wel et al. 2012), for member galaxies ($\Delta z \pm 0.15, R < 10''$; filled histogram), and for all galaxies in the GOODS-S field within $\Delta z \pm 0.15$ of the nebula redshift (open histogram, scaled down for clarity). The size of the PSF (top panel) and the Sérsic n values for exponential and De Vaucouleurs profiles (bottom panel) are indicated with dotted lines.